

Isothermal Phase Equilibria for Binary Hydrate Systems of Carbon Dioxide + Ethane and Carbon Dioxide + Tetrafluoromethane

Yuuki Matsui,[†] Yoshihiro Ogura,[†] Hiroshi Miyauchi,[†] Takashi Makino,[‡] Takeshi Sugahara,[†] and Kazunari Ohgaki^{*†}

Division of Chemical Engineering, Department of Materials Engineering Science, Graduate School of Engineering Science, Osaka University, 1-3 Machikaneyama, Toyonaka, Osaka 560-8531, Japan, and Department of Applied Chemistry, Kobe City College of Technology, 8-3 Gakuen-Higashi, Nishi-ku, Kobe 651-2194, Japan

The present paper reports isothermal three-phase equilibria (hydrate + aqueous + gas phases) for the carbon dioxide (CO₂) + ethane (C₂H₆) mixed-gas hydrate system at (274.15, 279.15, and 284.15) K and the carbon dioxide (CO₂) + tetrafluoromethane (CF₄) mixed-gas hydrate system at (274.15 and 279.15) K. None of the equilibrium pressure–composition curves of hydrate, aqueous, and gas phases shows discontinuity in the gradient. Both CO₂ + C₂H₆ and CO₂ + CF₄ mixed-gas hydrates are the structure-I hydrate under the present experimental conditions, which is supported by the results of in situ Raman spectroscopy.

Introduction

Gas hydrate is an inclusion compound, of which the host frameworks are formed by hydrogen-bonded water molecules. A guest molecule like hydrocarbons occupies a hydrate cage, which is a unit of the host framework. The unit cell of structure-I, one of the well-known hydrate structures, consists of two small cages (S-cage, pentagonal dodecahedron (5¹²)) and six large cages (M-cage, tetrakaidecahedron (5¹²6²)) with 46 water molecules. The thermodynamic properties and crystal structure of the simple gas hydrate mainly depend on guest species in addition to temperatures and pressures. For example, CO₂, C₂H₆, and CF₄ generate the structure-I hydrate¹ under the equilibrium conditions investigated in the present study.

Ohgaki and Inoue² have proposed the idea for CO₂ isolation on the sea floor by using gas hydrates. Liquid CO₂, which is injected onto the sea floor, forms CO₂ hydrate with seawater. At the sea floor deeper than 6000 m, the CO₂ hydrate is intermediate in density between liquid CO₂ and seawater. As a result, the CO₂ hydrate prevents liquid CO₂ from convecting upward from sea floor. The gas hydrate technology has a potential for the isolation of other green-house effect gases (N₂O, hydrofluorocarbon, perfluorocarbon, and SF₆) with CO₂. Ohgaki et al.³ have also proposed the natural-gas recovery process from the natural-gas hydrate sediments by the displacement of CH₄ to CO₂. Generally, natural gas contains C₂H₆, C₃H₈, and others, although the composition of natural gas depends on the source. The hydrates in the sediments change from CH₄ mixed-gas hydrates to CO₂ mixed-gas hydrates as a result of the displacement from CH₄ to CO₂. Then, thermodynamic properties of CO₂ mixed-gas hydrates as well as CH₄ mixed-gas hydrates are important for the gas hydrate related technologies. However, the quantity of information, especially the equilibrium compositions of hydrate and aqueous phases, about the CO₂ mixed-gas hydrate system is limited. In the present study, we have investigated isothermal phase equilibria for two CO₂ mixed-

gas hydrate systems under the three-phase (hydrate + aqueous + gas phases) equilibrium conditions by static temperature measurement and Raman spectroscopy. The one is the CO₂ + C₂H₆ system at (274.15, 279.15, and 284.15) K, and the other is the CO₂ + CF₄ system at (274.15 and 279.15) K. In addition, the crystal structure of mixed-gas hydrates has been identified by in situ Raman spectroscopy, on the basis of the comparison with Raman spectra of the guest and host molecules in structure-I and structure-II hydrates.

Experimental Section

The present experimental apparatus for phase equilibrium measurement and Raman spectroscopic analysis are the same as that of the previous works.^{4,5} Details of the experimental apparatus for the phase equilibrium measurement and Raman spectroscopic analysis have been described elsewhere.^{4,5} Equilibrium temperature was measured by a thermistor probe (model: Takara D-641) calibrated by a Pt resistance thermometer (25 Ω) defined by ITS-90. Equilibrium pressure was recorded by a pressure gauge (model: Valcom VPRT) calibrated by a RUSKA quartz Bourdon tube gauge.

Materials. C₂H₆ (mole purity: 0.999) was purchased from Takachiho Trading Co., Ltd. CO₂ (mole purity: 0.9999) and CF₄ (mole purity: 0.99999) were purchased from Neriki Gas Co., Ltd. The distilled water was obtained from Wako Pure Chemicals Industries, Ltd. All materials were used without further purification.

Phase Equilibrium Measurements. A gas mixture was introduced into an evacuated high-pressure cell. The contents were pressurized up to a desired pressure by supplying distilled water successively. The cell was immersed in a thermostatted bath for precise control of the temperature. A programming thermocontroller (model: Taitec CL-80R) circulated thermostatted water. Then, the mixed-gas hydrate was generated by agitation and cooling of the contents. A mixing bar was moved up-and-down by magnetic attraction from outside of the cell. The phase behavior was observed directly through a window attached to the cell. After the formation of the mixed-gas hydrate, the temperature was kept constant to establish the three-

* Corresponding author. Telephone and fax: +81-6-6850-6290. E-mail: ohgaki@cheng.es.osaka-u.ac.jp.

[†] Osaka University.

[‡] Kobe City College of Technology.

phase (hydrate + aqueous + gas phases) equilibrium condition. Small amounts of gas and aqueous phases were separately taken out under three-phase equilibrium conditions to analyze the equilibrium composition by means of gas chromatography (model: Shimadzu GC-14B with TCD detector). The uncertainties of equilibrium temperature, pressure, and composition were 0.02 K, 0.005 MPa, and 0.001, respectively.

The gas mixtures, which were released from quenched mixed-gas hydrate samples, were analyzed to measure the equilibrium composition in the hydrate phase. To prepare the mixed-gas hydrate for composition analysis, another high-pressure cell, pressure gauge, and thermocontroller were used.⁵ The generation of the mixed-gas hydrate sample and establishment of the three-phase equilibrium condition were performed by the same procedure mentioned above. After that, only the excess water in the high-pressure cell was sufficiently removed. Then, the mixed-gas hydrate was quenched at 253 K and taken out from the cell. The sample was allowed to dissociate under room temperature conditions, and the released mixed-gas was analyzed by using the same thermal conductivity detector/gas chromatograph (TCD-GC). The uncertainties of equilibrium temperature, pressure, and composition were 0.02 K, 0.02 MPa, and 0.001, respectively.

Raman Spectroscopic Analysis. The mixed-gas hydrate was generated by the same procedure as the phase equilibrium measurements. A thermocontroller (model: EYELA NCB-3100) circulated thermostatted water in the jacket of the high-pressure optical cell to control temperature. A ruby ball was enclosed in the cell to agitate the contents by low-frequency vibration from the outside. After the formation of the gas hydrate, the temperature was gradually increased and decreased to prepare hydrate single crystals at the three-phase coexisting state. After the single crystals were annealed to avoid metastability, the temperature was kept constant to establish the three-phase equilibrium condition. The uncertainties of equilibrium temperature, pressure, and composition were 0.02 K, 0.02 MPa, and 0.06, respectively.

The single crystal was analyzed under the three-phase equilibrium condition by in situ Raman spectroscopy by use of a laser Raman microprobe spectrometer with multichannel charge-coupled device (CCD) detector (model: Jobin-Yvon T64000). The Ar ion laser (wavelength: 514.5 nm, generation power: 100 mW), which was focused to 2 μm in spot diameter, was irradiated from the object lens onto the hydrate single crystal through the upper sapphire window. Integration time was varied from (150 to 300) s, depending on the intensity of Raman scattering. The CCD detector was maintained at 140 K by liquid N₂ for heat-noise reduction. The spectral resolution was 0.7 cm^{-1} . Raman peaks were calibrated with the Ne emission lines in the air. The crystal structure was identified by Raman shift corresponding to the enclathrated guest species.

In addition, the equilibrium composition of the hydrate phase was estimated from the Raman peak area by direct comparison of the quenched hydrate sample. To analyze equilibrium composition, we paid attention to the following Raman peaks: the Raman peak of the intramolecular C–C stretching vibration mode of C₂H₆ ($\tilde{\nu}_3 \sim 995 \text{ cm}^{-1}$),⁶ one of the Fermi-resonance peaks of CO₂ ($\tilde{\nu}_+ \sim 1388 \text{ cm}^{-1}$),⁶ and the intramolecular C–F stretching vibration mode of CF₄ ($\tilde{\nu}_1 \sim 908 \text{ cm}^{-1}$).⁶

Results and Discussion

CO₂ + C₂H₆ Mixed-Gas Hydrate System. Phase equilibrium data obtained from the phase equilibrium measurements and Raman spectroscopic analysis at (274.15, 279.15, and 284.15)

Table 1. Isothermal Phase Equilibria for the CO₂ (1) + C₂H₆ (2) Mixed-Gas Hydrate System at (274.15, 279.15, and 284.15) K

p/MPa	x_1	x_1'	y_1	z_1 (TCD-GC)
$T/\text{K} = 279.15$				
0.997	0		0	0
1.013	0.257		0.044	
1.029	0.420		0.067	
1.051	0.642		0.124	
1.108	0.705		0.220	
1.141	0.811		0.263	
1.15 ^a				0.283
1.264	0.902		0.400	
1.343	0.936		0.483	
1.385	0.944		0.506	
1.49 ^a				0.543
1.542	0.965		0.608	
1.618	0.968		0.667	
1.73 ^a				0.699
1.835	0.982		0.779	
1.921	0.986		0.791	
1.984	0.988		0.829	
2.00 ^a				0.792
2.287	0.994		0.942	
2.543	1		1	1
$T/\text{K} = 274.15$				
0.530	0		0	0
0.545	0.339		0.047	
0.566	0.626		0.118	
0.572	0.653		0.131	
0.595	0.768		0.180	
0.621	0.815		0.245	
0.654	0.868		0.294	
0.684	0.902		0.384	
0.700	0.915		0.403	
0.742	0.931		0.478	
0.771	0.940		0.515	
0.807	0.951		0.568	
0.852	0.963		0.621	
0.894	0.967		0.665	
0.965	0.977		0.736	
1.044	0.983		0.797	
1.100	0.988		0.844	
1.196	0.992		0.901	
1.287	0.996		0.950	
1.385	1		1	1
$T/\text{K} = 284.15$				
1.913	0		0	0
1.970	0.570		0.097	
2.003	0.650		0.144	
2.120	0.822		0.250	
2.207	0.854		0.319	
2.265	0.888		0.364	
2.425	0.918		0.445	
2.628	0.942		0.553	
2.840	0.960		0.621	
2.990	0.970		0.649	
3.121	0.974		0.684	
3.171	0.976		0.698	
3.300	0.979		0.723	
3.542	0.983		0.777	
3.962	0.987		0.858	
4.173	0.993		0.886	
4.602	0.995		0.929	
4.870	0.996	0.973		
5.680	0.997	0.979		

^a Equilibrium data obtained from the TCD-GC measurement of the quenched hydrate sample.

K are summarized in Tables 1 and 2, respectively. Figure 1 shows isothermal phase equilibria for the CO₂ + C₂H₆ mixed-gas hydrate system at 279.15 K. Three-phase equilibrium curves are in good agreement with the calculated equilibrium relations of CSM Gem,¹ although there is slight difference between the measured and the calculated equilibrium curves of the hydrate

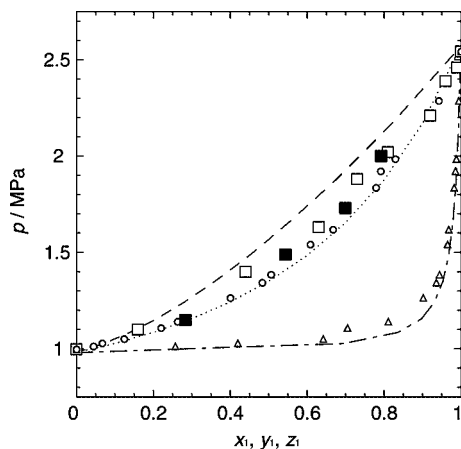


Figure 1. Isothermal phase equilibria for the CO₂ (1) + C₂H₆ (2) mixed-gas hydrate system at 279.15 K. Symbols stand for the experimental data in the present study: □, hydrate phase (Raman); ●, hydrate phase (TCD-GC); ○, gas phase; △, aqueous phase. The curves represent the equilibrium relations obtained by CSM Gem:¹ dashed line, hydrate phase; dotted line, gas phase; chained line, aqueous phase.

Table 2. Isothermal Pressure–Composition Relations (Based on Raman Spectroscopic Analysis) for the CO₂ (1) + C₂H₆ (2) Mixed-Gas Hydrate System at (274.15, 279.15, and 284.15) K

p/MPa	z_1 (Raman)
$T/\text{K} = 279.15$	
1.10	0.16
1.40	0.44
1.63	0.63
1.88	0.73
2.02	0.81
2.21	0.92
2.39	0.96
2.46	0.99
$T/\text{K} = 274.15$	
0.54	0.05
0.69	0.34
0.77	0.43
1.02	0.71
1.14	0.84
1.27	0.92
1.32	0.96
$T/\text{K} = 284.15$	
2.06	0.14
2.67	0.48
2.84	0.58
3.34	0.70
3.57	0.77
4.05	0.85
4.25	0.88
5.11	0.93

phase. Both equilibrium curves of the hydrate phase measured with Raman and TCD-GC methods are laid in the concentration region slightly higher than calculated one. The equilibrium pressure increases monotonically with an increase of equilibrium CO₂ composition. The equilibrium CO₂ compositions in hydrate, gas, and aqueous phases increase in this order under isobaric conditions.

Each equilibrium curve does not have any discontinuity in gradient, which indicates that no structural transition of hydrates occurs at 279.15 K. Figure 2 shows typical Raman spectra of the CO₂ + C₂H₆ mixed-gas hydrates. The symbol of $\tilde{\nu}$ stands for Raman shift. The single Raman peak derived from the intramolecular C–C stretching vibration of the enclathrated C₂H₆ molecule was detected at 1000 cm⁻¹. The Raman shift is similar to that corresponding to the C₂H₆ molecule encaged in the M-cage of structure-I.^{5,7,8} Therefore, the single peak detected

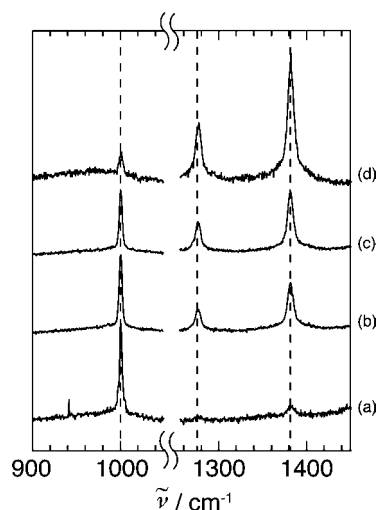


Figure 2. Raman spectra of the intramolecular C–C stretching vibration (1000 cm⁻¹) of the C₂H₆ and the symmetric stretching vibration (1275 cm⁻¹) and overtone of bending vibration (1381 cm⁻¹) of the CO₂ in the CO₂ (1) + C₂H₆ (2) mixed-gas hydrate at 279.15 K. (a) $p = 1.10$ MPa, $z_1 = 0.16$; (b) $p = 1.63$ MPa, $z_1 = 0.63$; (c) $p = 1.88$ MPa, $z_1 = 0.73$; (d) $p = 2.39$ MPa, $z_1 = 0.96$.

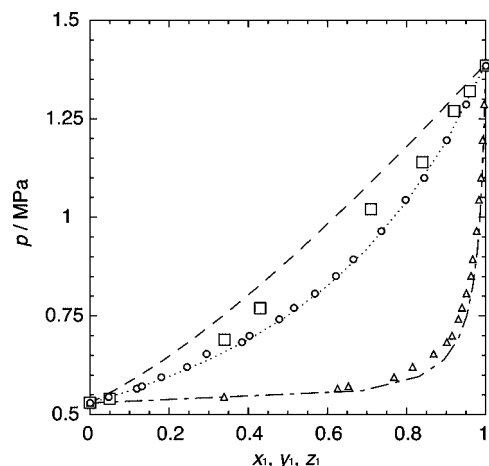


Figure 3. Isothermal phase equilibria for the CO₂ (1) + C₂H₆ (2) mixed-gas hydrate system at 274.15 K. Symbols stand for the experimental data in the present study: □, hydrate phase (Raman); ○, gas phase; △, aqueous phase. The curves represent the equilibrium relations obtained by CSM Gem:¹ dashed line, hydrate phase; dotted line, gas phase; chained line, aqueous phase.

at 1000 cm⁻¹ indicates that the crystal structure of the CO₂ + C₂H₆ mixed-gas hydrate is structure-I in the whole composition range of 279.15 K. C₂H₆ molecule cannot occupy the S-cage of the CO₂ + C₂H₆ mixed-gas hydrates at the pressures. In addition, the Raman peaks of the enclathrated CO₂ molecule were detected at (1275 and 1381) cm⁻¹ by the Fermi-resonance effect.⁹ These wavenumbers are in good agreement with those of CO₂ in the simple and binary structure-I CO₂ hydrates.^{4,10–12}

Isothermal phase equilibria for the CO₂ + C₂H₆ mixed-gas hydrate system at (274.15 and 284.15) K are shown in Figures 3 and 4, respectively. The symbol of rhombus in Figure 4 stands for the equilibrium composition (x') of CO₂ in the liquid CO₂ phase. Other symbols are the same as those of Figure 1. Isothermal phase behaviors at (274.15 and 284.15) K are similar to that at 279.15 K. Therefore, the pressure–composition relations and Raman spectra indicate that the crystal structure of the CO₂ + C₂H₆ hydrate is structure-I in the whole composition range and the temperature range from (274.15 to

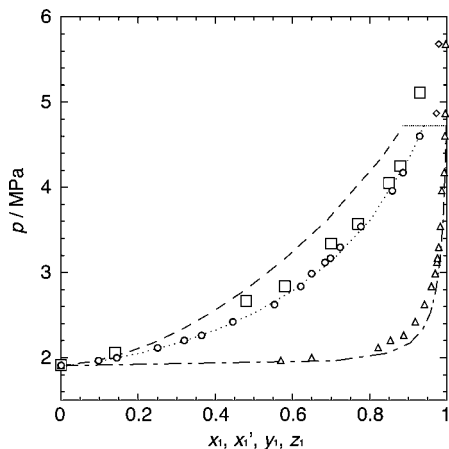


Figure 4. Isothermal phase equilibria for the CO_2 (1) + C_2H_6 (2) mixed-gas hydrate system at 284.15 K. Symbols stand for the experimental data in the present study: \square , hydrate phase (Raman); \circ , gas phase; \triangle , aqueous phase; \diamond , liquid CO_2 phase. The horizontal line around 4.7 MPa represents the four-phase equilibrium relation of hydrate + gas + aqueous + liquid CO_2 phases. The curves represent the equilibrium relations obtained by CSM Gem:¹ dashed line, hydrate phase; dotted line, gas phase; chained line, aqueous phase.

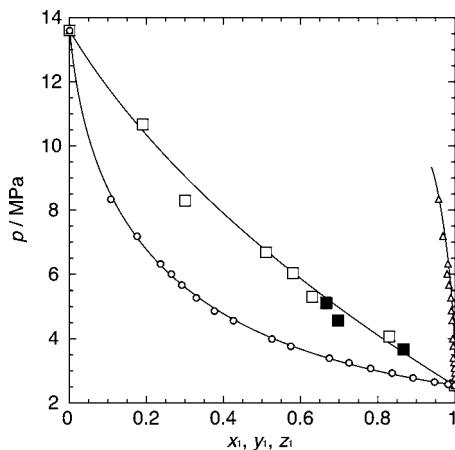


Figure 5. Isothermal phase equilibria for the CO_2 (1) + CF_4 (2) mixed-gas hydrate system at 279.15 K. Symbols stand for the experimental data in the present study: \square , hydrate phase (Raman); \blacksquare , hydrate phase (TCD-GC); \circ , gas phase; \triangle , aqueous phase.

284.15) K. In addition, at 284.15 K, the gas phase disappears, and instead the liquid CO_2 phase appears in the pressure range over 4.65 MPa. That is, another three-phase equilibrium state (hydrate + aqueous + liquid CO_2 phases) is established. The four-phase equilibrium point (hydrate + aqueous + gas + liquid CO_2 phases) is estimated around $p = (4.7 \pm 0.1)$ MPa, $x_1 = 0.99 \pm 0.01$, $x_1' = 0.97 \pm 0.01$, $y_1 = 0.95 \pm 0.02$, and $z_1 = 0.91 \pm 0.03$. The present equilibrium relations are in good agreement with the literature relations.¹³

CO_2 + CF_4 Mixed-Gas Hydrate System. Isothermal phase equilibria for the CO_2 + CF_4 mixed-gas hydrate system at (279.15 and 274.15) K are shown in Figures 5 and 6, respectively. Phase equilibrium data obtained from the phase equilibrium measurements and Raman spectroscopic analysis are summarized in Tables 3 and 4, respectively. At 279.15 K, the equilibrium pressure of the simple CF_4 hydrate is 13.6 MPa.¹⁴ The equilibrium pressure of mixed-gas hydrate system decreases monotonically with an increase of equilibrium CO_2 composition. Unlike the CO_2 + C_2H_6 mixed-gas hydrate system, the CO_2 mole fractions of gas, hydrate, and aqueous phases

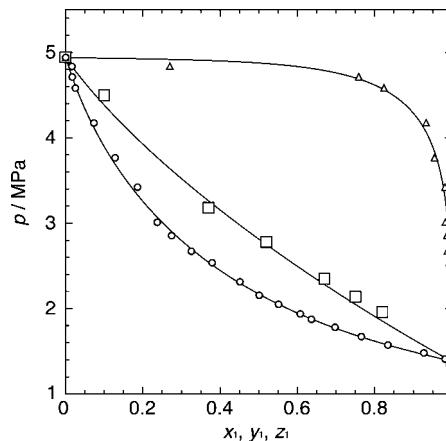


Figure 6. Isothermal phase equilibria for the CO_2 (1) + CF_4 (2) mixed-gas hydrate system at 274.15 K. Symbols stand for the experimental data in the present study: \square , hydrate phase (Raman); \circ , gas phase; \triangle , aqueous phase.

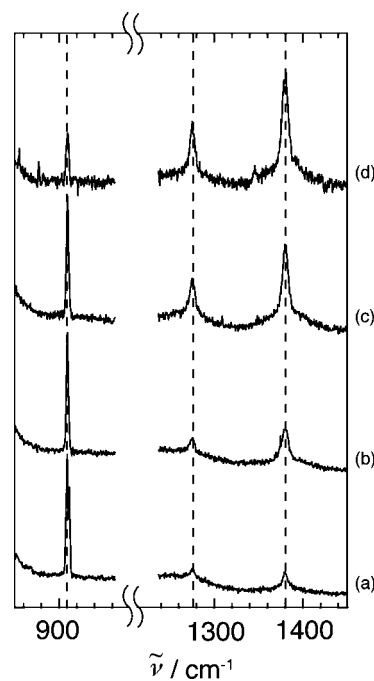


Figure 7. Raman spectra of the intramolecular C–F stretching vibration (908 cm^{-1}) of the CF_4 and the symmetric stretching vibration (1275 cm^{-1}) and overtone of bending vibration (1381 cm^{-1}) of the CO_2 in the CO_2 (1) + CF_4 (2) mixed-gas hydrate at 279.15 K. (a) $p = 10.67$ MPa, $z_1 = 0.19$; (b) $p = 6.69$ MPa, $z_1 = 0.51$; (c) $p = 5.30$ MPa, $z_1 = 0.63$; (d) $p = 4.07$ MPa, $z_1 = 0.83$.

increase in this order under isobaric conditions. The equilibrium relations in Figures 5 and 6 show smooth curves like the CO_2 + C_2H_6 hydrate system.

Raman spectra obtained from the CO_2 + CF_4 mixed-gas hydrate at 279.15 K are shown in Figure 7. The single Raman peak derived from the intramolecular C–F stretching vibration of the enclathrated CF_4 molecule was detected at 908 cm^{-1} . The Raman shift of CF_4 is in good agreement with that in the M-cage of the simple CF_4 and CH_4 + CF_4 structure-I hydrates.^{14,15} Furthermore, the Raman peaks of the CO_2 molecule in the hydrate phase reveal that the structure of the CO_2 + CF_4 mixed-gas hydrate is structure-I. Isothermal phase behavior at 274.15 K is similar to that at 279.15 K. Therefore,

Table 3. Isothermal Phase Equilibria for the CO₂ (1) + CF₄ (2) Mixed-Gas Hydrate System at (274.15 and 279.15) K

<i>p</i> /MPa	<i>x</i> ₁	<i>y</i> ₁	<i>z</i> ₁ (TCD-GC)
<i>T</i> /K = 279.15			
2.543	1	1	1
2.584	1.000	0.982	
2.655	1.000	0.947	
2.787	1.000	0.891	
2.934	1.000	0.837	
3.079	0.999	0.781	
3.255	0.998	0.725	
3.394	0.996	0.674	
3.67 ^a			0.867
3.767	0.996	0.574	
3.995	0.995	0.525	
4.567	0.993	0.425	
4.57 ^a			0.697
4.868	0.991	0.376	
5.12 ^a			0.666
5.277	0.990	0.329	
5.678	0.985	0.291	
6.016	0.980	0.264	
6.334	0.982	0.236	
7.194	0.969	0.175	
8.348	0.958	0.107	
13.6 ^b	0	0	0
<i>T</i> /K = 274.15			
1.385	1	1	1
1.412	1.000	0.982	
1.483	1.000	0.927	
1.576	0.999	0.834	
1.673	0.999	0.765	
1.784	0.998	0.697	
1.877	0.998	0.636	
1.940	0.998	0.607	
2.053	0.996	0.551	
2.159	0.996	0.501	
2.316	0.995	0.451	
2.539	0.993	0.379	
2.673	0.988	0.325	
2.857	0.987	0.274	
3.013	0.983	0.237	
3.423	0.982	0.186	
3.768	0.955	0.128	
4.176	0.933	0.073	
4.585	0.824	0.025	
4.715	0.759	0.017	
4.838	0.270	0.016	
4.945	0	0	0

^a Equilibrium data obtained from the TCD-GC measurement of the quenched hydrate sample. ^b Ref 15.

the crystal structure of the CO₂ + CF₄ hydrate is also structure-I under the present conditions of (274.15 and 279.15) K.

Conclusion

Isothermal phase equilibria for the two mixed-gas hydrate systems containing CO₂ have been investigated by means of gas chromatography and Raman spectroscopy. The isothermal equilibrium pressures for the CO₂ + C₂H₆ ((274.15 to 284.15) K) and CO₂ + CF₄ ((274.15 to 279.15) K) systems change monotonically with a rise of equilibrium CO₂ composition. Phase equilibria and Raman spectra indicate that no structural transition of hydrates occurs at the present experimental pressures and temperatures in the CO₂ + C₂H₆ and CO₂ + CF₄ hydrate systems.

Table 4. Isothermal Pressure–Composition Relations (Based on Raman Spectroscopic Analysis) for the CO₂ (1) + CF₄ (2) Mixed-Gas Hydrate System at (274.15 and 279.15) K

<i>p</i> /MPa	<i>z</i> ₁ (Raman)
<i>T</i> /K = 279.15	
4.07	0.83
5.30	0.63
6.04	0.58
6.69	0.51
8.32	0.30
10.67	0.19
<i>T</i> /K = 274.15	
1.96	0.82
2.14	0.75
2.35	0.67
2.78	0.52
3.18	0.37
4.50	0.10

Literature Cited

- (1) Sloan, E. D.; Koh, C. A. *Clathrate Hydrates of Natural Gases*, 3rd ed.; Taylor Group, CRC Press: Boca Raton, FL, 2007.
- (2) Ohgaki, K.; Inoue, Y. A proposal for gas storage on the ocean floor using gas hydrates. *Kagaku Kogaku Ronbunshu* **1991**, *17*, 1053–1055.
- (3) Ohgaki, K.; Takano, K.; Sangawa, H.; Matsubara, T.; Nakano, S. Methane exploitation by carbon dioxide from gas hydrates - phase equilibria for CO₂-CH₄ mixed hydrate system. *J. Chem. Eng. Jpn.* **1996**, *29*, 478–483.
- (4) Makino, T.; Ogura, Y.; Matsui, Y.; Sugahara, T.; Ohgaki, K. Isothermal phase equilibria and structural phase transition in the carbon dioxide + cyclopropane mixed-gas hydrate system. *Fluid Phase Equilib.* **2009**, *284*, 19–25.
- (5) Hashimoto, S.; Sasatani, A.; Matsui, Y.; Sugahara, T.; Ohgaki, K. Isothermal phase equilibria for methane + ethane + water ternary system containing gas hydrates. *Open Thermodyn. J.* **2008**, *2*, 100–105.
- (6) Shimanouchi, T. *Tables of Molecular Vibrational Frequencies*, consolidated, Vol. I; National Bureau of Standards Department of Commerce: Washington, DC, 1972.
- (7) Morita, K.; Nakano, S.; Ohgaki, K. Structure and stability of ethane hydrate crystal. *Fluid Phase Equilib.* **2000**, *169*, 167–175.
- (8) Subramanian, S.; Kini, R. A.; Dec, S. F.; Sloan, E. D., Jr. Evidence of structure II hydrate formation from methane + ethane mixtures. *Chem. Eng. Sci.* **2000**, *55*, 1981–1999.
- (9) Wright, R. B.; Wang, C. H. Density effect the Fermi resonance in gaseous CO₂ by Raman scattering. *J. Chem. Phys.* **1973**, *58*, 2893–2895.
- (10) Nakano, S.; Moritoki, M.; Ohgaki, K. High-pressure phase equilibrium and Raman microprobe spectroscopic studies on the CO₂ hydrate system. *J. Chem. Eng. Data* **1998**, *43*, 807–810.
- (11) Uchida, T.; Takagi, A.; Mae, S.; Kawabata, J. Dissolution mechanisms of CO₂ molecules in water containing CO₂ hydrate. *Energy Convers. Manage.* **1997**, *38*, 307–312.
- (12) Uchida, T.; Ikeda, I. Y.; Takeya, S.; Kamata, Y.; Ohmura, R.; Nagao, J.; Zatspeina, O. Y.; Buffett, B. A. Kinetics and stability of CH₄-CO₂ mixed gas hydrates during formation and long-term storage. *Chem. Phys. Chem.* **2005**, *6*, 646–654.
- (13) Adisasmito, S.; Sloan, E. D. Hydrates of hydrocarbon gases containing carbon dioxide. *J. Chem. Eng. Data* **1992**, *37*, 343–349.
- (14) Sugahara, K.; Yoshida, M.; Sugahara, T.; Ohgaki, K. High-pressure phase behavior and cage occupancy for the CF₄ hydrate system. *J. Chem. Eng. Data* **2004**, *49*, 326–329.
- (15) Kunita, Y.; Makino, T.; Sugahara, T.; Ohgaki, K. Raman spectroscopic studies on methane + tetrafluoromethane mixed-gas hydrate system. *Fluid Phase Equilib.* **2007**, *251*, 145–148.

Received for review January 29, 2010. Accepted April 21, 2010. The authors are grateful to the Division of Chemical Engineering, Graduate School of Engineering Science, Osaka University for the scientific support by “Gas-Hydrate Analyzing System (GHAS).”

JE100097X